IOP Publishing and International Atomic Energy Agency Nuclear Fusion
Nucl. Fusion **52** (2012) 063006 (8pp) doi:10.1088/0029-5515/52/6/063006

Sawtooth control using electron cyclotron current drive in ITER demonstration plasmas in DIII-D

I.T. Chapman[1], R.J. La Haye[2], R.J. Buttery[2], W.W. Heidbrink[3], G.L. Jackson[2], C.M. Muscatello[3], C.C. Petty[2], R.I. Pinsker[2], B.J. Tobias[4] and F. Turco[5]

[1] Euratom/CCFE Fusion Association, Culham Science Centre, Abingdon, OX14 3DB, UK
[2] General Atomics, PO Box 85608, San Diego, CA 92186-5608, USA
[3] University of California, Irvine, CA 92697, USA
[4] Princeton Plasma Physics Laboratory, Princeton, NJ 08543, USA
[5] Department of Applied Physics and Applied Mathematics, Columbia University, New York, USA

E-mail: ian.chapman@ccfe.ac.uk

Received 16 December 2011, accepted for publication 22 March 2012
Published 17 April 2012
Online at stacks.iop.org/NF/52/063006

Abstract
Sawtooth control using electron cyclotron current drive (ECCD) has been demonstrated in ITER-like plasmas with a large fast ion fraction, wide $q = 1$ radius and long uncontrolled sawtooth period in DIII-D. The sawtooth period is minimized when the ECCD resonance is just inside the $q = 1$ surface. Sawtooth destabilization using driven current inside $q = 1$ avoids the triggering of performance-degrading neoclassical tearing modes (NTMs), even at much higher pressure than required in the ITER baseline scenario. Operation at $\beta_N = 3$ without 3/2 or 2/1 NTMs has been achieved in ITER demonstration plasmas when sawtooth control is applied using only modest ECCD power. Numerical modelling qualitatively confirms that the achieved driven current changes the local magnetic shear sufficiently to compensate for the stabilizing influence of the energetic particles in the plasma core.

1. Introduction

It is well known that tokamak macroscopic instabilities are primarily driven by steepening gradients in the current density or the pressure. Sawtooth oscillations are the manifestation of the $n = m = 1$ internal kink mode, one such magnetohydrodynamic (MHD) instability, characterized by quasi-periodic collapses in the temperature and density in the plasma core (here, m and n are the poloidal and toroidal periodicity of the wave). However, minority populations of super thermal ions can delay the onset of these instabilities, thereby improving confinement properties of tokamaks and allowing steeper pressure and current gradients to develop. The presence of fusion-born alpha particles in ITER is predicted to significantly lengthen the time between consecutive sawtooth crash events [1–4]. This means that when the sawtooth crash occurs in the presence of stabilizing fast ions it is often more violent and more likely to trigger neoclassical tearing modes (NTMs), leading to a degradation in pressure and thus in fusion performance. Indeed, long period sawteeth are empirically shown to be more likely to trigger NTMs [5]. Consequently there is much interest in control schemes which can maintain small, frequent sawtooth crashes which avoid seeding deleterious NTMs.

When electron cyclotron resonance heating (ECRH) is applied to the plasma, a change in the local current density occurs due to the change in the temperature, and subsequent change in the conductivity. When applied in the vicinity of the resonant surface associated with the internal kink mode, $q = 1$, this has the consequence of moving the radius of the $q = 1$ surface, r_1, and changing the magnetic shear at $q = 1$, s_1, thus affecting the likelihood of a sawtooth crash. Here, the safety factor is $q = \mathrm{d}\psi_\phi/\mathrm{d}\psi_\theta$ and the magnetic shear is $s = r/q\,\mathrm{d}q/\mathrm{d}r$ with ψ_θ and ψ_ϕ the poloidal and toroidal magnetic fluxes respectively. Furthermore, by adding a toroidal component to the wave vector of the launched EC waves, an ancillary electron cyclotron driven current results either parallel (co-electron cyclotron current drive (ECCD)] or anti-parallel (counter-ECCD) to the ohmic current, enhancing the potential to change s_1. Figure 1 shows the case when ECCD is applied inside the $q = 1$ surface, where the local change in current density results in an increase in the gradient of the q-profile at $q = 1$. Here the blue current density profile is a typical H-mode profile

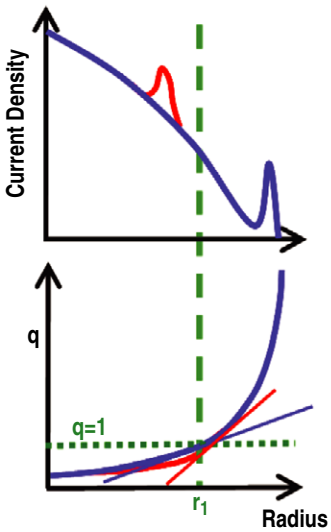

Figure 1. When ECCD is applied, a local perturbation to the current density profile (red, where blue is the usual H-mode profile) results in the $q = 1$ radius moving outwards and the magnetic shear increasing.

with bootstrap peak near the edge, whereas the red curve shows the ancillary electron cyclotron driven current inside $q = 1$. The control of sawtooth oscillations in tokamaks through noninductively driven currents has been demonstrated on a number of machines [6–13], and consequently has been included in the design of the sawtooth control system for ITER [14, 15]. The history of sawtooth control using current drive is reviewed in reference [16]. It is worth noting that the control of sawteeth for NTM prevention using ECCD has been demonstrated directly on ASDEX Upgrade: Reference [17] shows that NTMs are avoided at high pressure by complete suppression of the sawteeth using co-ECCD just outside the $q = 1$ surface. Concomitant with the end of the gyrotron pulse, a sawtooth crash occurred and an NTM was triggered, resulting in a substantial degradation of the plasma performance. However, it is widely accepted that sawteeth cannot be avoided throughout an ITER discharge, and so a similar demonstration of avoidance of NTMs with deliberately accelerated frequent sawteeth is required. Furthermore, experiments in JET demonstrated sawtooth destabilization and consequent avoidance of NTMs, even at high β_N in H-mode [18, 19]. However, these experiments used ICRH as the control actuator, rather than ECCD as reported here and planned for ITER. Recently, the mechanism of sawtooth control when using ICRH has been explained by tailoring the phase space of the fast ion distribution [20, 21], so direct comparison between the JET ICRH results and ECCD sawtooth control is complex.

The fundamental trigger of the sawtooth crash is thought to be the onset of an $m = n = 1$ mode, although the dynamics of this instability are constrained by many factors including not only the macroscopic drive from ideal MHD, but collisionless kinetic effects related to high energy particles [22–24] and thermal particles [25, 26], as well as non-ideal effects localized in the narrow layer around $q = 1$. A heuristic model predicts that a sawtooth crash will occur in the presence of energetic ions when various criteria are met [1, 27, 28], with the defining one usually given in terms of a critical magnetic shear determined either by the pressure gradient, $s_1 > s_{\rm crit}(\omega_{*\rm i})$, or by the mode potential energy, written as

$$s_1 > \max\left[s_{\rm crit} = \frac{4\delta W}{\xi_0^2 \epsilon_1^2 R B^2 c_\rho \hat{\rho}}, s_{\rm crit}(\omega_*)\right] , \qquad (1)$$

where c_ρ is a normalization coefficient of the order of unity, $\hat{\rho} = \rho_{\rm i}/r_1$, $\rho_{\rm i}$ is the ion Larmor radius, R is the major radius, B is the toroidal field, $\epsilon_1 = r_1/R$, ξ_0 is the magnetic perturbation at the magnetic axis and $\omega_{*\rm i}$ is the ion diamagnetic frequency. The change in the kink mode potential energy is defined such that $\delta W = \delta W_{\rm core} + \delta W_{\rm h}$ and $\delta W_{\rm core} = \delta W_{\rm f} + \delta W_{\rm KO}$ where $\delta W_{\rm KO}$ is the change in the mode energy due to the collisionless thermal ions [25], $\delta W_{\rm h}$ is the change in energy due to the fast ions and $\delta W_{\rm f}$ is the ideal fluid mode drive [29].

The remaining concern about current drive control is whether changes in s_1 can overcome the stabilization arising from the presence of energetic particles. In ITER, the fusion-born α particles are likely to give rise to a large stabilizing potential energy contribution, $\delta W_{\rm h}$ in the internal kink mode dispersion relation, which coupled with the small $\hat{\rho}$ in the denominator of equation (1) means the critical shear to drive the internal kink mode unstable is increased. The result is that the change in the magnetic shear may need to be prohibitively large in order to compete with the kinetic stabilization, especially if the fast ions arising from concurrent ion cyclotron resonance heating (ICRH) and neutral beam injection (NBI) heating exacerbate the situation [4]. Consequently, recent experiments have focussed on destabilizing sawteeth using ECCD in the presence of energetic particles. Sawtooth destabilization of long period sawteeth induced by ICRH generated core fast ions with energies $\geqslant$0.5 MeV was achieved in Tore Supra, even with modest levels of ECCD power [30, 31]. Similarly, ECCD destabilization has also been achieved in the presence of ICRH accelerated NBI ions in ASDEX Upgrade [32] as well as with normal NBI fast ions in ASDEX Upgrade [7] and JT-60U [33]. Despite these promising results, destabilization of so-called monster sawteeth—that is to say sawteeth with periods longer than the energy confinement time, and hence saturated central plasma temperature—in the presence of a significant population of highly energetic particles at high $\beta_{\rm h}$ (where $\beta_{\rm h}$ is the fast ion pressure divided by the magnetic pressure) has yet to be demonstrated in ITER-like conditions. This paper aims to address this issue. In section 2 sawtooth control in ITER demonstration plasmas is demonstrated in DIII-D for long sawteeth in the presence of energetic NBI ions. After demonstrating the optimal deposition for ECCD in order to destabilize the sawteeth, the improvement in fusion performance with sawtooth control is discussed in section 3. In section 4 the effect of changing the magnetic shear is compared with the stabilizing drive from the fast ions using numerical simulation, before the implications of this work are discussed in section 5.

2. Sawtooth control using ECCD in the presence of energetic ions

ITER baseline demonstration plasmas have been developed on DIII-D [34] to match many of the anticipated operating parameters for ITER [35]: the plasma cross-section matches

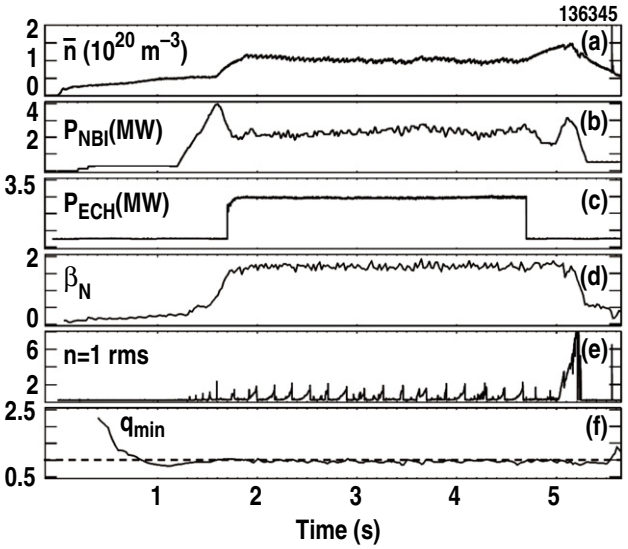

Figure 2. Time traces for a DIII-D shot 136345 which is a typical ITER demonstration plasma with $I_p = 1.45$ MA, $B_T = 1.92$ T and $W_h/W_f \approx 0.2$. (*a*) The density is relatively constant and allows the pedestal collisionality to match that expected in ITER. (*b*) The NBI power (modulation averaged over 100 ms here) is in β_N feedback. (*c*) The ECH power is directed off-axis to keep the density low. (*d*) $\beta_N = 1.8$ is kept constant and ITER baseline level. (*e*) The plasma sawtooths throughout and (*f*) q_{min} is just below one, resulting in a broad low-shear region expected in ITER ELMy H-modes.

the ITER design scaled by a factor of 3.7; the plasma confinement and normalized pressure match the target values for ITER, namely $H_{98,y2} = 1.0$ and $\beta_N = 1.8$, where $H_{98,y2}$ is the energy confinement enhancement factor, $\beta_N = \beta a B_0/I_p$ where a is the minor radius, I_p (MA) is the plasma current, $\beta = 2\mu_0\langle p\rangle/B_0^2$ and $\langle\cdots\rangle$ represents an averaging over the plasma volume and p is the plasma pressure; the field ($B_T = 1.9$ T) and current ($I_p = 1.45$ MA) are set such that $I/aB = 1.415$ which equates to $I_p = 15$ MA in ITER; the resultant safety factor at the 95% flux surface, $q_{95} = 3.1$ is close to the ITER design value of 3.0; the density is set in such a way that the pedestal collisionality is matched to that expected in ITER; and finally, there is a broad low-shear region of the safety factor resulting in $\rho_1 = 0.35$ approaching the $\rho_1 = 0.45$ value expected in ITER (notwithstanding the large error bar associated with this in the transport modelling). A typical ITER demonstration plasma is illustrated in figure 2. The plasma experiences monster sawteeth throughout, with an average sawtooth period of $\tau_{st} = 265$ ms compared with an energy confinement time of $\tau_E = 220$ ms. Scaling the sawtooth period by the resistive diffusion time [36] and r_1, this period is roughly equivalent to 50 s in ITER, which is approaching the expected critical sawtooth period likely to seed NTMs [5].

Tearing mode activity is present throughout, with a benign $m/n = 4/3$ tearing mode persisting throughout most of the discharge, though not affecting confinement significantly, and a $m/n = 2/1$ tearing mode triggered by a sawtooth crash near the end of the flat-top (after the off-axis ECCD near $q = 2$ is turned off). Constant off-axis broad-deposition electron cyclotron heating (ECH) is required to attain low density, likely to work by driving an electron-temperature gradient mode in the locality of the EC resonance, and to avoid a disruptive 2/1 mode. The off-axis ECCD near $q = 2$ is broad (in the sense that it is broader than islands present in the plasma) and not modulated, meaning that it is not optimized for stabilizing any NTMs occurring in the plasma. In the plasmas reported here, only co-current on-axis NBI is used. Whilst DIII-D is equipped with both counter-current and off-axis neutral beams, both have been shown numerically and empirically to destabilize the internal kink mode and result in shorter sawtooth periods [37–40]. Given that the aim of this paper is to demonstrate the efficacy of ECCD destabilization in the presence of fast ions, any ancillary sources of sawtooth destabilization are omitted. This has the consequence that these DIII-D plasmas have relatively high injected torque and thus rotate faster than the toroidal frequency expected in ITER. It should be noted that this differential rotation is likely to influence the potential coupling between the 1/1 internal kink mode associated with the sawteeth and higher m/n NTMs.

An important difference between these plasmas and the ITER baseline scenario is the fraction of energetic particles. The NBI induced fast ions constitute approximately 15% of the stored energy, whereas the fusion-born alpha particles in ITER, combined with NBI and ICRH fast ions, result in a fast ion fraction ($\langle\beta_h\rangle/\langle\beta\rangle$) in ITER approaching 45% (β_α from reference [41], β_{NBI} from reference [42]).

The ECCD resonance was swept by performing very slow ramps in the toroidal field, commensurate with slow ramps in plasma current to keep the q-profile constant. These ramps, which are typically only 6% variation over 2500 ms, are necessarily slow since the sawtooth period was sometimes longer than half a second and the ramps must proceed sufficiently slowly that the optimal deposition location for sawtooth destabilization can be inferred. Figure 3 shows the EC driven current predicted by the TORAY-GA code [43, 44]. Both the off-axis EC absorption location and the amplitude of the driven current is relatively insensitive to the sweep in the toroidal field because the rays are nearly tangent to the flux surface due to the ray refraction at large minor radius. Conversely, the 12% difference in toroidal field between discharges 145688 and 145692 results in the on-axis EC resonance location moving in the range $\rho_{EC} \in [0.17, 0.35]$, which spans a significant region both inside and outside the $q = 1$ radius considering the relatively narrow ECCD width. The fact that the off-axis EC deposition is relatively invariant ensures that no adverse changes to current density profile affect tearing stability at higher m/n rational surfaces and allow low target density to be retained throughout to achieve a high fast ion fraction.

The sawtooth behaviour in typical ITER demonstration plasmas in DIII-D is shown in discharge 145861 in figure 4. Here the 1.4 MW of ECH is directed off-axis to achieve a low density and thus $W_h/W_{total} = 0.12$. The sawteeth are regular with an average sawtooth period of 260 ms and the β_N is kept fixed by feedback on the auxiliary NBI power during the very small I_p, B_T ramp. Also shown is a comparison shot with core ECCD applied inside $q = 1$, with the sweep in field and current moving the deposition from well inside $q = 1$ towards r_1, but not crossing $q = 1$. It is clear that the average sawtooth period drops significantly and the shortest sawteeth are 125 ms, less than half the uncontrolled period. This is a clear demonstration

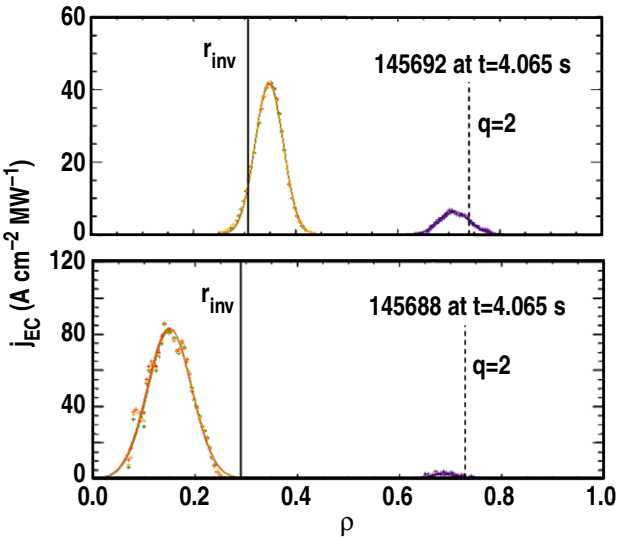

Figure 3. The electron cyclotron driven current and heating profiles for discharge 145692 when the core deposition is centred at $\rho = 0.35$ and for shot 145688 when the core ECCD is at $\rho = 0.17$. Despite the large sweep in core EC deposition, the off-axis deposition remains almost unchanged.

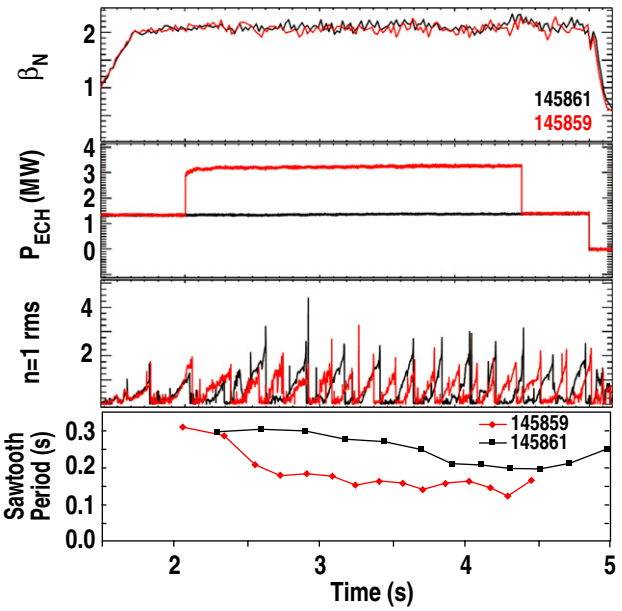

Figure 4. The normalized beta, ECH power and $n = 1$ mode activity for shots 145861 (no core ECCD) and 145859 (with core ECCD). It is clear that the sawtooth frequency increases by approximately 50% when there is ECCD just inside $q = 1$.

of robust sawtooth control in the presence of a significant population of energetic particles. In this discharge 1.5 MW of ECCD (compared with $P_{\text{aux}} = 5$ MW) was required to reduce the sawtooth period by 50%.

By performing a series of sweeps in field and current, the deposition location of the ECCD can be moved from near the magnetic axis to well outside the $q = 1$ surface, noting that the inversion radius does move slightly as the ECCD resonance moves. The field and current sweeps were performed in both directions so that any hysteresis in the sawtooth period would be evident. Figure 5 shows the sawtooth period as a function of

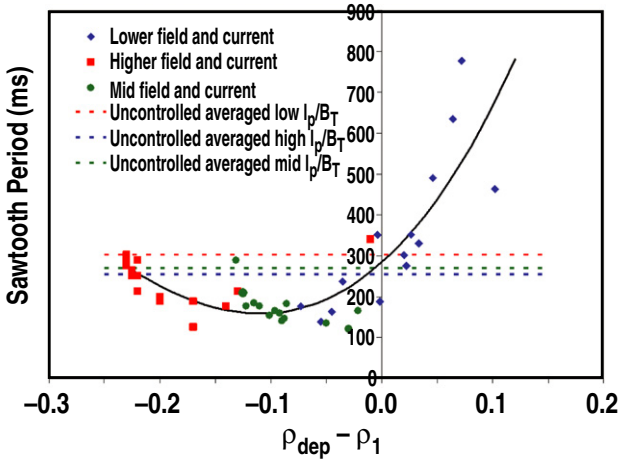

Figure 5. The sawtooth period as a function of the difference of the $q = 1$ radius and the peak EC deposition radius, shown with a best-fit third order polynomial to guide the eye. It is evident that the sawtooth period is minimized when the ECCD is localized a small distance inside the $q = 1$ surface, as expected. This is a clear demonstration of such behaviour in H-mode plasmas with a large fast ion fraction.

the difference between the EC resonance location calculated by TORAY-GA and the inversion radius, here considered as representative of the $q = 1$ surface. The inversion radii are calculated by looking for inversion on the electron cyclotron emission diagnostic, which has a radial resolution of 1 cm, the soft x-ray diagnostic which has resolution of 2.5 cm and finally by matching the mode frequency to the rotation profile from charge exchange recombination spectroscopy. It is clear that the minimum in sawtooth period occurs when the ECCD has a resonance just inside the $q = 1$ surface, as one would expect [8, 16], since this maximizes the local magnetic shear at $q = 1$. That this strong correlation—which has previously been shown in L-mode and low power plasmas [7, 8, 12, 45–47]—persists in the presence of energetic ions is encouraging and shows that ECCD is an applicable actuator in ITER plasmas. The optimal destabilization occurs for a broad range of deposition, $\rho_{\text{dep}} - \rho_1 \in [-0.2, -0.03]$.

3. Improved performance using ECCD sawtooth control in ITER demonstration plasmas

As discussed in section 2, the ITER demonstration plasmas in DIII-D are susceptible to performance-degrading tearing modes (either 3/2 or 2/1), even at the relatively modest normalized pressure of $\beta_{\text{N}} = 1.8$. That is not to say that tearing modes are ubiquitous in these plasmas, but they are common depending upon subtle nuances of the current profile [48], even more so at low applied torque. The most deleterious instability is the $m/n = 2/1$ NTM which is usually triggered by an edge-localized mode (ELM) or a sawtooth crash that triggers an ELM or by a sawtooth alone. Whilst stabilization of the 2/1 NTM has been shown to lead to much improved performance in DIII-D [49], it is preferable to avoid triggering the NTMs by utilizing sawtooth control. NTM control requires ECCD power near $q = 2$ which means that it does not usefully heat the core of the plasma, whereas the ECCD for sawtooth control described in section 2 is inside $q = 1$. Furthermore,

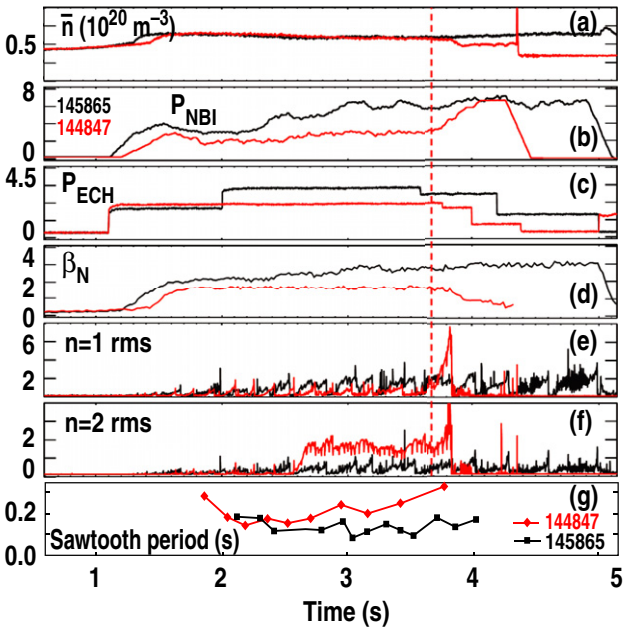

Figure 6. The density, NBI power, ECH power, normalized beta and $n = 1$ and $n = 2$ mode activity in discharges 144847 (red, no sawtooth control) and 145865 (black, with sawtooth control). Whilst a 2/1 NTM is triggered at 3.7 s after a sawtooth crash in 144847, when $\beta_N = 1.8$, much higher performance is achieved for much longer with sawtooth control, allowing $\beta_N \approx 3$.

ECCD efficiency drops with increasing radius, exemplified by the current densities achieved for different locations given similar input power in figure 3, making core ECCD even more preferable. Extrapolating this to ITER, avoidance of NTMs by sawtooth control is far preferable for fusion yield, Q [50].

The scans in field and current allowed the optimal resonance location for the ECCD to be inferred from figure 5. The relative insensitivity of the minimum in sawtooth period to the exact resonance location with respect to $q = 1$ means that sawtooth control in DIII-D can be achieved without real-time steering of the EC launcher mirrors. Indeed, this insensitivity allows the resonance location to be fixed and the pressure to be increased, whilst retaining frequent, controlled sawteeth despite the enhanced Shafranov shift at higher β. We now choose the resonance location and set the field and current accordingly so that $\rho_{dep} - \rho_1 \approx -0.1$, then increase the auxiliary NBI power piece-wise in β_N feedback to increase the pressure and examine the efficacy of the sawtooth control. Figure 6 shows two very similar discharges in DIII-D, one without core ECCD and one with optimized ECCD for sawtooth control. In the absence of sawtooth control, discharge 144847 develops a 2/1 NTM triggered by a sawtooth crash at $\beta_N = 1.8$. This in itself is a paradigm of the importance of sawtooth control in the baseline scenario in ITER: This demonstration plasma matches most ITER parameters, and yet a 2/1 NTM is triggered, degrading confinement irreparably. This happens despite the fact that the fast ion fraction is less than half of that expected in ITER, which is likely to exacerbate the situation, pointing towards the need to prevent the NTM seeding. Shot 145865 is a demonstration of exactly this. Using only 1.5 MW of core ECCD inside $q = 1$, the internal kink mode is driven unstable and the sawteeth are small and frequent. The plasma pressure is steadily increased to the point that $\beta_N = 3.0$ and 2/1 NTMs are avoided throughout. The application of core ECCD meant that DIII-D plasmas were able to operate well in excess of the baseline normalized pressure foreseen in ITER reproducibly. Whilst the ECCD is applied throughout the discharge, it not only heats the plasma core as well as controlling the sawteeth, but its application allows access to much higher pressures, extrapolating to a significant increase in Q.

It should be noted that, as discussed in section 2, in order to achieve the low density, and thus high fast ion fraction desired in these ITER-like plasmas, off-axis ECCD is required near $q = 2$. This off-axis ECCD is broadly deposited and not modulated, and therefore not optimized for NTM control. Indeed, as exhibited in figure 6, when the sawtooth control is not applied, the off-axis ECCD does little to affect the triggering and subsequent growth of $m/n = 2/1$ NTMs. The small driven current from this off-axis ECCD will change very slightly at higher β_N as the Shafranov shift is enhanced, and therefore, it is possible that this small change in the current profile could affect tearing stability directly. However, the over-riding conclusion which persists is that this higher β is only accessible with the core sawtooth control which gives rise to sufficiently small sawteeth to avoid triggering NTMs, even at lower β_N.

The controlled sawteeth come about because the local increase in the magnetic shear at $q = 1$ afforded by the electron cyclotron driven current significantly destabilizes the 1/1 internal kink mode. This drive for the 1/1 mode can be seen clearly in the root-mean-square amplitude of the Fourier spectrogram of fluctuations measured on outboard midplane magnetic probe measurements shown in figure 7. In the absence of core ECCD, the sawtooth precursor mode is weak and intermittent and the sawtooth period is long. However, in discharge 145692, the increase in shear drives the 1/1 mode unstable according to equation (1), resulting in a strong, continuous perturbation in the plasma.

4. Modelling the effect of ECCD in high performance, high fast ion fraction plasmas

The effect of driving localized current on the stability of the internal kink mode has been assessed using linear stability analysis. Whilst such linear analysis cannot be used to infer anything directly about the nonlinear sawtooth period, it is still useful as a guide to internal kink stability, and indicative of the sawtooth behaviour. Indeed, it has been used to provide insight into empirical observation of sawtooth phenomenology on MAST [51], TEXTOR [52], JET [37, 38] and ASDEX Upgrade [40].

The reconstructed fixed-boundary equilibria are generated using the HELENA code [53], taking as input the current density profile from EFIT constrained by the motional Stark effect diagnostic and with a correction for the radial electric field. The pressure profile is taken from the Thomson scattering diagnostic, whilst the plasma boundary also comes from EFIT. Whilst the equilibrium is static, the linear MHD stability analysis using MISHKA-F [54] includes the effect of toroidal rotation perturbatively. This assumption is appropriate at very sub-sonic flow speeds present in these relatively low injected

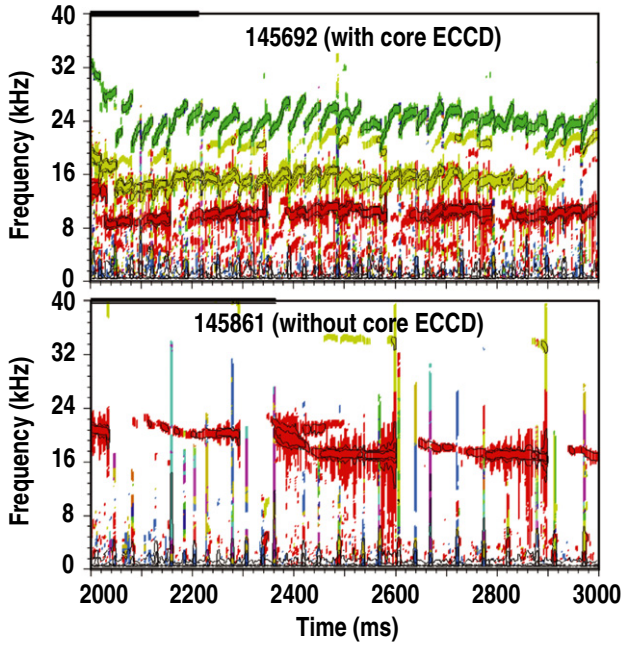

Figure 7. The magnetic spectrogram for discharges 145861 (no sawtooth control) and 145692 (with core ECCD sawtooth control) at the same plasma pressure. When sawtooth control is applied, the $n = 1$ mode is driven more unstable with strong precursor mode activity and higher coupled harmonics observed throughout.

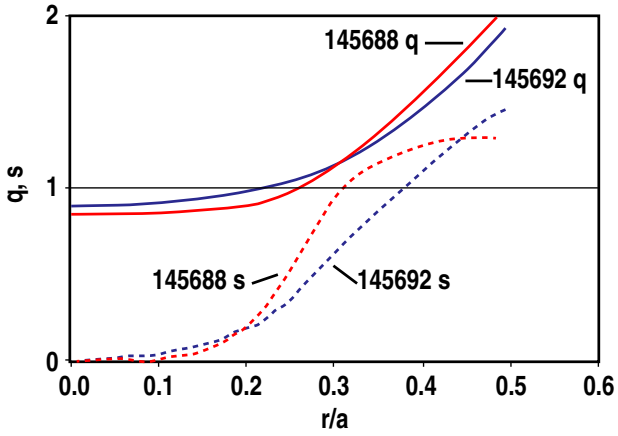

Figure 8. The MSE-constrained EFIT safety factor (solid) and shear (dashed) profiles just before a sawtooth crash for 145688 at $t = 2.465$ s when the EC resonance is inside the initial $q = 1$ position, resulting in an increase in r_1 and s_1 compared with the q-profile for shot 145692 at $t = 4.305$ s when the EC resonance is well outside $q = 1$.

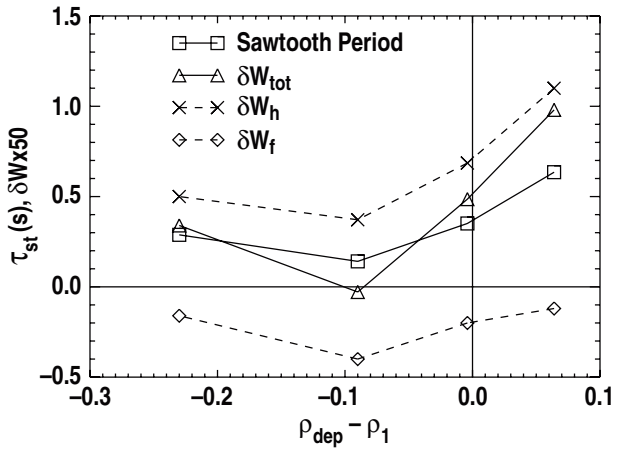

Figure 9. The sawtooth period as a function of the deposition peak of ECCD with respect to the $q = 1$ radius for timeslices in four different DIII-D discharges. The trend in sawtooth period is replicated by the change in the potential energy of the internal kink mode, $\delta W_{\rm tot}$, underpinned by the change in the magnetic shear and $q = 1$ radius due to local ECCD altering both $\delta W_{\rm h}$ and $\delta W_{\rm f}$.

torque plasmas [55, 56]. The rotation profile is taken from the charge exchange recombination spectroscopy diagnostic.

The effect of the fast ions on internal kink stability is analysed using the Monte Carlo drift kinetic HAGIS code [57]. HAGIS simulates the interaction between the perturbation taken from MISHKA-F and the energetic particle distribution taken from the TRANSP code [58]. Here TRANSP predicts a neutron rate which matches the experimentally measured neutron rate very well. The spectral shape and profile shapes of the beam ion distribution predicted by TRANSP have also been compared with the fast ion distribution measured by the vertically viewing fast ion D-alpha (FIDA) diagnostic [59]. Whilst the calculated FIDA signals [60] are larger than those measured by the FIDA diagnostic, the profiles and spectra give good confidence that the TRANSP beam ion distribution is reasonable.

A typical effect of the localized ECCD on the q-profile is illustrated in figure 8. In discharge 145692 at $t = 4.305$ s, the ECCD resonance is outside the $q = 1$ radius, leading to a long sawtooth period. In this case, the $q = 1$ surface is at $r_1 = 0.22a$ and the local magnetic shear is only $s_1 = 0.22$. Conversely, when the ECCD resonance is just inside the $q = 1$ surface, as is the case for discharge 145688 at $t = 2.465$ s, then the resonant surface is moved outwards by 18% to $r_1 = 0.26a$ and the magnetic shear increases by 200% to $s_1 = 0.66$.

The effect of changing the local magnetic shear is assessed by calculating the change in the potential energy of the $n = 1$ internal kink mode which enters into the critical magnetic shear required for a sawtooth to occur, as given by equation (1). The fluid drive for the mode, $\delta W_{\rm f}$ is calculated by MISHKA-F including the stabilizing effect of the toroidal rotation, whilst the stabilizing effect from the core fast ions, $\delta W_{\rm h}$, resulting from the NBI is calculated using HAGIS. Figure 9 shows the sawtooth period for four DIII-D discharges for different $\rho_{\rm dep} - \rho_1$, which have very different magnetic shear and radial positions of the $q = 1$ surface. It is clear that when the resonance is a short distance inside ρ_1, the fluid drive for the $n = m = 1$ internal kink is maximized because the EC driven current increases both the magnetic shear and r_1. As well as driving the internal kink, the stabilizing effect of the fast ions is diminished due to the normalization of $\delta \hat{W}_{\rm h}$ in equation (1) by the local magnetic shear. Here the $\delta \hat{W}_{\rm h}$ is calculated using the fast ion distribution from discharge 145692 throughout, though the neutral beam heating is the same in all shots so this is a reasonable approximation. Whilst linear stability calculations cannot be used to infer the sawtooth period, which is naturally dominated by nonlinear processes, it is indicative of sawtooth stability. Furthermore, the fact that the change in potential energy of the internal kink, $\delta W_{\rm tot}$, correlates strongly with the

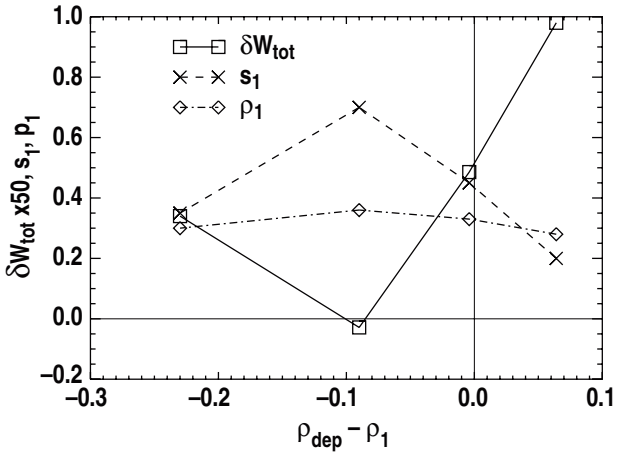

Figure 10. The change in the potential energy of the kink mode for the same four DIII-D sawteeth as shown in figure 10. Also shown is s_1 and ρ_1 for these four different EC resonance locations. It is clear that the change in δW arises from increasing both s_1 and ρ_1. It should be noted that δW is larger (more stable) for $\rho_{\rm dep}$ nearest ρ_1 than for the most on-axis resonance despite the higher magnetic shear because the $q = 1$ radius is expanded by the local ECCD compared with the on-axis resonance.

sawtooth period gives confidence that the dominant physics is captured in the modelling.

It should be noted that whilst the change in the local magnetic shear is the predominant driver in destabilizing the internal kink mode, the variation in the radial position of the $q = 1$ surface resulting from the ancillary noninductive current drive also influences stability. This is exemplified by figure 10 which shows that δW is larger (more stable) for $\rho_{\rm dep}$ nearest ρ_1 than for the most on-axis resonance despite the higher magnetic shear because the $q = 1$ radius is expanded by the local ECCD compared with the on-axis resonance. As r_1 increases, $\delta W_{\rm h}$ also increases markedly due to a greater number of energetic beam ion trajectories passing inside the $q = 1$ surface, and so stabilizing the kink mode [16].

5. Discussion and conclusions

The ITER ELMy H-mode baseline scenario is designed to be sawtoothing. The significant population of fast ions arising from the NBI, ICRH, and of course, the fusion born α particles, is expected to result in very long sawtooth periods, potentially of the order of 100 s [1, 61, 62]. Empirical scaling suggests that such long sawteeth are likely to trigger deleterious NTMs [5] and so some sawtooth control is required. Whilst NTM suppression is planned for ITER, direct avoidance by sawtooth control is preferable for optimizing the fusion yield. As well as heating the core plasma when ECCD is applied inside $q = 1$ for sawtooth control, the ECCD efficiency is far greater near the core than near the $q = 2$ surface. However, given the small ion Larmor radius and large positive $\delta W_{\rm h}$ resulting from the energetic ion populations, equation (1) suggests that sawtooth control using current drive schemes is likely to be more challenging. The results presented here show that not only is ECCD control possible in ITER-like plasmas, but that it can predicate much higher performance than forecast to be required to meet $Q = 10$ in ITER whilst still avoiding NTMs.

Sawtooth destabilization has been achieved with modest ECCD power in the presence of a significant population of fast ions. The fact that a modest level of injected EC power could result in such a dramatic change in the sawtooth behaviour, despite the strong stabilizing contribution of the energetic beam ions, suggests that the destabilizing effect of increased local magnetic shear may be stronger than reference [1] suggests. This is the case, for instance, in the stability criteria for the drift tearing mode in reference [28] where a fourth order dependence on s_1 appears. Whilst these energetic particles represent up to approximately 20% of the plasma pressure, this is still much less than expected in ITER, and definitive demonstration of the effectiveness of ECCD does require a larger fast ion fraction in future studies. The sawtooth period is minimized when the EC resonance is just inside the $q = 1$ surface, which results in the largest increase in the local magnetic shear. The minimum in sawtooth period is relatively insensitive to the exact deposition location once the EC resonance is inside the $q = 1$ surface, as predicted to be the case in ITER in transport analysis too [63]. These experiments give credence to the numerical assessment that 13MW of ECCD will be an effective control actuator in ITER plasmas [63, 64]. Finally, substantially enhanced fusion performance has been demonstrated here with sawtooth control, giving hope that similar performance could be achieved without triggering NTMs in ITER if necessary in order to reach the $Q = 10$ goal.

Acknowledgments

This work was supported in part by the RCUK Energy Programme under grant EP/I501045, the European Communities under the contract of Association between EURATOM and CCFE and the US Department of Energy under DE-FC02-04ER54698, SC-G903402, and DE-AC02-09CH11466. The views and opinions expressed herein do not necessarily reflect those of the European Commission.

References

[1] Porcelli F., Boucher D. and Rosenbluth M. 1996 *Plasma Phys. Control. Fusion* **38** 2163
[2] Chapman I.T. *et al* 2007 *Plasma Phys. Control. Fusion* **49** B385
[3] Hu B., Betti R. and Manickam J. 2006 *Phys. Plasmas* **13** 112505
[4] Chapman IT *et al* 2011 *Plasma Phys. Control. Fusion* **53** 124003
[5] Chapman I.T. *et al* 2010 *Nucl. Fusion* **50** 102001
[6] Ahkaev V.V. *et al* 1995 *Nucl. Fusion* **35** 369
[7] Mück A., Goodman T.P., Maraschek M., Pereverez G., Ryter F. and Zohm H. 2005 *Plasma Phys. Control. Fusion* **47** 1633
[8] Angioni C., Goodman T., Henderson M. and Sauter O. 2003 *Nucl. Fusion* **43** 455
[9] Sauter O. *et al* 2001 *Phys. Plasmas* **8** 2199
[10] Ikeda Y. *et al* 2002 *Nucl. Fusion* **42** 375
[11] Pinsker R.I., Luce T.C. Petty, C.C., Prater R., La Haye R.J., Lazarus E.A., Wong K.-L. and Sauter O. 2003 *Bull. Am. Phys. Soc.* **48** 128
[12] Westerhof E. *et al* 2003 *Nucl. Fusion* **43** 1371
[13] Lennholm M. *et al* 2007 *17th Top. Conf. on Radio Frequency Power in Plasmas (Clearwater, Florida, USA)* vol 933 p 401 http://proceedings.aip.org/resource/2/apcpcs/933/1?isAuthorized=no
[14] Henderson M. *et al* 2007 *Fusion Eng. Des.* **82** 454

[15] Darbos C. *et al* 2009 Radio frequency power in plasmas *Proc. 18th Top. Conf. (Gent, Belgium)* vol 1187 p 531 http://proceedings.aip.org/resource/2/apcpcs/1187/1?isAuthorized=no
[16] Chapman I.T. 2011 *Plasma Phys. Control. Fusion* **53** 003001
[17] Maraschek M. *et al* 2005 *Nucl. Fusion* **45** 1369
[18] Sauter O. *et al* 2002 *Phys. Rev. Lett.* **88** 105001
[19] Westerhof E. *et al* 2002 *Nucl. Fusion* **42** 1324
[20] Graves J.P. *et al* 2010 *Nucl. Fusion* **50** 052002
[21] Graves J.P. *et al* 2012 *Nature Commun.* **3** 624
[22] Porcelli F. 1991 *Plasma Phys. Control. Fusion* **33** 1601
[23] Graves J.P., Chapman I.T., Coda S., Eriksson L.G. and Johnson T. 2009 *Phys. Rev. Lett.* **102** 065005
[24] Graves J.P., Sauter O. and Gorelenkov N. 2003 *Phys. Plasmas* **10** 1034
[25] Kruskal M. and Oberman C. 1958 *Phys. Fluids* **1** 275
[26] Fogaccia G. and Romanelli F. 1995 *Phys. Plasmas* **2** 227
[27] Sauter O. *et al* 1998 *Theory of Fusion Plasmas, Proc. Joint Varenna–Lausanne International Workshop (Varenna, Italy)* (New York: AIP) p 403
[28] Cowley S.C., Kulsrud R.M. and Hahm T.S. 1986 *Phys. Fluids* **29** 3230
[29] Bussac M.N., Pellat R., Edery D. and Soule J.L. 1975 *Phys. Rev. Lett.* **35** 1638
[30] Lennholm M. *et al* 2009 *Phys. Rev. Lett.* **102** 115004
[31] Lennholm M. *et al* 2009 *Fusion Sci. Technol.* **55** 45
[32] Igochine V. *et al* 2011 *Plasma Phys. Control. Fusion* **53** 022002
[33] Isayama A. *et al* 2002 *J. Plasma Fusion Res. Ser.* **5** 324
[34] Doyle E.J. *et al* 2010 *Nucl. Fusion* **50** 075005
[35] ITER Physics Basis 2007 *Nucl. Fusion* **47** S1
[36] Park W. and Monticello D. 1990 *Nucl. Fusion* **30** 2413
[37] Chapman I.T. *et al* 2007 *Phys. Plasmas* **14** 070703
[38] Chapman I.T., Jenkins I., Budny R.V., Graves, J.P., Pinches S.D. Saarelma S. and JET EFDA Contributors 2008 *Plasma Phys. Control. Fusion* **50** 045006
[39] Chapman I.T. *et al* 2009 *Nucl. Fusion* **49** 035006
[40] Chapman I.T. *et al* 2009 *Phys. Plasmas* **16** 072506
[41] Budny R.V. 2002 *Nucl. Fusion* **42** 1383
[42] Asunta O. *et al* http://users.tkk.fi/∼tkurki/RIPLOS_FR_Nov2008.pdf
[43] Cohen R.H. 1988 *Nucl. Fusion* **28** 1871
[44] Matsuda K. 1989 *IEEE Trans. Plasma Sci.* **PS-17** 6
[45] Snider R.T., Content D., James R., Lohr J., Mahdavi M.A., Prater R. and Stallard B. 1989 *Phys. Fluids* B **1** 404
[46] Hanada K. *et al* 1991 *Phys. Rev. Lett.* **66** 1974
[47] Pietrzyk Z.A. *et al* 1999 *Nucl. Fusion* **39** 587
[48] Turco F. and Luce T.C. 2010 *Nucl. Fusion* **50** 095010
[49] Prater R. *et al* 2007 *Nucl. Fusion* **47** 371
[50] Sauter O., Henderson, M.A., Ramponi G., Zohm H. and Zucca C. 2010 *Plasma Phys. Control. Fusion* **52** 025002
[51] Chapman I.T., Hender T.C., Saarelma S., Sharapov S.E., Akers R.J. and Conway N.J. 2006 *Nucl. Fusion* **46** 1009
[52] Chapman I.T., Pinches S.D., Koslowski H.R., Liang Y., Kramer-Flecken A. and de Bock M. 2008 *Nucl. Fusion* **48** 035004
[53] Huysmans G.T.A. *et al* 1991 *Proc. CP90 Conf. on Comput. Phys.* p 371
[54] Chapman I.T., Huysmans G.T.A., Mikhailovskii A.B. and Sharapov S.E. 2006 *Phys. Plasmas* **13** 062511
[55] Chapman I.T., Graves J.P. and Wahlberg C. 2010 *Nucl. Fusion* **50** 025018
[56] Wahlberg C., Chapman I.T. and Graves J.P. 2009 *Phys. Plasmas* **16** 112512
[57] Pinches S.D. *et al* 1998 *Comput. Phys. Commun.* **111** 133
[58] Budny R.V. *et al* 1992 *Nucl. Fusion* **32** 429
[59] Luo Y., Heidbrink W.W., Burrell K.H., Kaplan D.H. and Gohil P. 2007 *Rev. Sci. Instrum.* **78** 033505
[60] Heidbrink W.W., Liu D., Luo Y., Ruskov E. and Geiger B. 2011 *Commun. Comput. Phys.* **10** 716
[61] Jardin S.C., Bell M.G. and Pomphrey N. 1993 *Nucl. Fusion* **33** 371
[62] Onjun T. and Pianroj Y. 2009 *Nucl. Fusion* **49** 075003
[63] Zucca C. *et al* 2008 *Theory of Fusion Plasmas, Joint Varenna–Lausanne Theory Conf. (Varenna, Italy)* vol 1069 p 361 http://proceedings.aip.org/dbt/dbt.jsp?KEY=APCPCS&Volume=1069&Issue=1
[64] Graves J.P., Chapman I.T., Coda S., Johnson T., Lennholm M., Paley J.I., Sauter O. and JET-EFDA Contributors 2011 *Fusion Sci. Technol.* **59** 539